Iranica Journal of Energy & Environment 4 {(3) Geo-hazards and Civil Engineering)}: 186-198, 2013
ISSN 2079-2115
IJEE an Official Peer Reviewed Journal of Babol Noshirvani University of Technology
DOI: 10.5829/idosi.ijee.2013.04.03.03

BUT

Seismic Behavior Assessment of RBS and AW-RBS Moment Resistant Connections with Double I-Beam

Morteza Naghipour and Saleh Mohammad Ebrahimzadeh Sepasgozar

Department of Civil Engineering, Babol Noshirvani University of Technology

(Received: January 29, 2013; Accepted in Revised Form: March 18, 2013)

Abstract: Today Steel moment resistance connections are the most common type of connections that are widely used in steel structures and certainly play a significant role in retrofitting, reliability and economic benefits. It is used also for improvement of the quality and useful life cycle of buildings. Considering the motions importance and after the Northridge earthquake, the invention of RBS connection was a turning point in resistant steel moment connections. This research observes the seismic behavior of the RBS connection with reduced section of flange and a new AW- RBS with reduced section of web in a double section beams that are applicable in Iran. These observations are performed using ABQUS finite elements software. Many models are implemented under cycle loads and ductility. Energy absorption and plastic behavior in the reduced section were observed. Among the studied connections, AW- RBS with the least resistance and stiffness decrement had bearded 8% off the rotation of the story. These models have acceptable behavior in cyclic loads.

Key words: RBS connections · Accordion effect · Double beam · Plastic hinge · Hysteresis behavior

INTRODUCTION

The 1994 Northridge earthquake revealed serious damage to conventional beam-to-column connections, which were formerly known as ductile moment connections. The Northridge and Kobe earthquakes in 1995 have prompted the design profession and construction industry to investigate and revise material, design and workmanship criteria for these frames. Since then, a great deal of research has been conducted on the existing moment connections to find deficiencies and to improve their cyclic behavior. The first approach provides a beam-to-column connection stronger than the beam itself, through reinforcing a short portion of the beam near the column by the use of cover plates, ribs, haunches or side plates. The second approach however, referred as Reduced Beam Section (RBS), such connection can be achieved by reducing flanges area at a specific distance from the beam-to-column connection, called Reduced Beam Section (RBS) or by reducing web area by introducing large opening into the web, called Reduced Web Section (RWS).

As a schematic example of a steel beam-to-column moment frame connection Plumier was the first to introduce the trapezoidal cut RBS [1].

The straight-cut, the tapered-cut, referred to as teardrop [2], a slight modification [3] and the radius-cut (circular, radiused), while two more rather marginal types have also been reported. All Types of RBS configurations are depicted in Figure 1. The behavior of beams with corrugated webs was investigated in the United States by Rothwell [4], Sherman and Fisher [5], Libove [6, 7], Easly [8], Wu and Libove [9] and Hussain and Libove [10]. Similar studies were conducted in Britain by Harrison [11], in Hungary by Korashy and Varga [12], in Sweden by Bergfelt and Liva-Aravena [13] and in Germany by Lindner and Aschinger [14] and Scheer *et al*. [15].

Beams with corrugated webs have been manufactured in Japan [16] and also used in building in the United State, Europe and in bridges in France [17, 18]. A summary of the research and developments in the area of corrugated web beams and girders was reported by Elgaaly and Dagher [19]. Recently, Chan *et al*. [20] investigated the effect of web corrugation on the beam's

Corresponding Author: Morteza Naghipour, Department of Civil Engineering, Babol Noshirvani University of Technology. E-mail: m-naghi@nit.ac.ir.

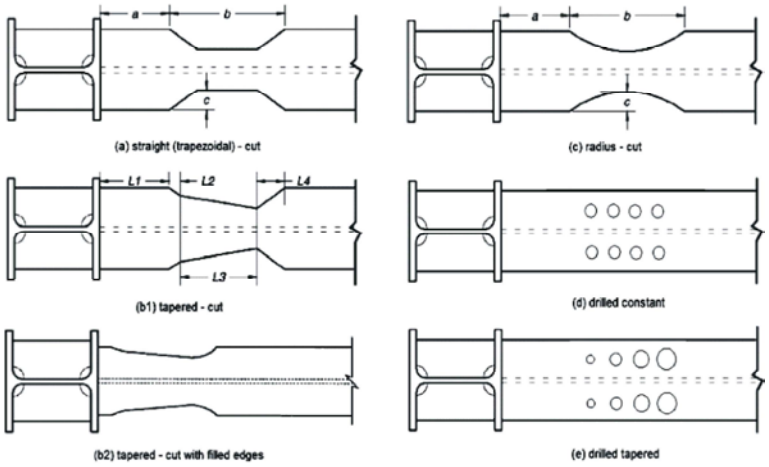

Fig. 1: Types of RBS configurations

strength and flange buckling. Finite elements approaches were used for modeling in beams with flat web, vertically and horizontally corrugated webs. The vertically corrugated web provided a stronger support against the flange buckling, compared to girders with horizontally corrugated-web and flat-web types.

The behavior of connection with corrugated webs that have called a new type of RBS connection, "Accordion Web RBS (AW-RBS)" was investigated in Iran by Mirghaderi [21]. The analytical and experimental results, the inelastic rotations of the connection are mostly provided by reliable and ductile rotation at the reduced region rather than in the connection plates or panel zone.

In this paper, the general purpose finite element package ABAQUS was used [22]. AW-RBS connection is presented by analytical method of this type of connection and extended on deep beams with double I-beam that commonly work goes on in resistance frame in the Iran.

Finite Element Model

Preprocessing Method: Today one of the research methods that has significant contributions to scientific advances. The technique used in most fields of engineering, is numerical simulation. Numerical simulation using simulation software, a significant advantage in terms of cost, time and reliability of the test is in reality. This research study through numerical simulations via ABAQUS finite element software simulation was performed.

Model Setup: In this study, 10 rigid flexural connections were compared. The types of cutting RBS were radius-cut, tapered-cut and Accordion-Web RBS connection that weak the web of a beam, with double I-beam, which is removed in a limited zone near the column. In this study, in particular, four L-shape folded plates are employed. The connection models were firstly designed then the models converted into ABAQUS. A samples model of the connection is shown in Figure 2.

In this research eleven 2/3 scale specimens, almost identical are used. The column height is 2.2 m and the beam length is 1.6 m for each side.

The specimens consisted of cruciform interior connection subassemblies with beams attached to the column opposite faces, based on AISC [23].

The profile connections study at this paper is shown in Table 1. The subassemblies are extracted from interior joints of moment frames, deflected under lateral loads. In moment frames the inflection points are formed near the mid-span of beams and mid-height of columns. By this assumption, the inflection points of moment frames are considered to be the ends of subassembly beams and columns with hinged supports. The proportioning of specimens is governed by the maximum load capacity and the stroke of the actuator. The specimens are designed to satisfy the strong-column weak-beam criterion to ensure a plastic mechanism of the beam. As double I-beams are used ordinarily for specimens -way moment frames in Iran. Regarding large torsional stiffness and strength of such beams, a double I-beam was selected to eliminate the relevant instabilities and failure modes as well as to focus more on the connection behavior.

Design Procedure of AW-RBS Connections: The design procedure of RBS and AW-RBS connections are based on AISC seismic provisions [23]. The geometric design parameters are the distance from the column face to the

Table 1: Details of connections

Models	Beam	Column	Doubler plate	Continuse plate	Corrugated plate	RBS		
						a	b	c
RBS with Radius-cut	2 X IPE180	IPB260	yes	yes	No	0.7 b_{fb}	0.8 d_{fb}	0.18 b_{fb}
RBS with triangular-cut	2 X IPE180	IPB260	yes	yes	No	0.7 b_{fb}	0.8 d_{fb}	0.18 b_{fb}
RBS with Trapezoidal-cut	2 X IPE180	IPB260	yes	yes	No	0.7 b_{fb}	0.8 d_{fb}	0.18 b_{fb}
RBS with Corrugated plate	2 X IPE180	IPB260	yes	yes	4 Corrugated plate	0.7 b_{fb}	0.8 d_{fb}	0.18 b_{fb}
RBS with Corrugated plate	2 X IPE180	IPB260	yes	yes	2 Corrugated plate only inside	0.7 b_{fb}	0.8 d_{fb}	0.18 b_{fb}
RBS with Corrugated plate	2 X IPE180	IPB260	yes	yes	2 Corrugated plate only outside	0.7 b_{fb}	0.8 d_{fb}	0.18 b_{fb}
RBS with Corrugated plate	2 X IPE140	IPB260	yes	yes	4 Corrugated plate	0.7 b_{fb}	0.8 d_{fb}	0.18 b_{fb}
RBS with Corrugated plate	2 X IPE160	IPB260	yes	yes	4 Corrugated plate	0.7 b_{fb}	0.8 d_{fb}	0.18 b_{fb}
RBS with Corrugated plate	2 X IPE200	IPB260	yes	yes	4 Corrugated plate	0.7 b_{fb}	0.8 d_{fb}	0.18 b_{fb}
RBS with Corrugated plate	2 X IPE220	IPB260	yes	yes	4 Corrugated plate	0.7 b_{fb}	0.8 d_{fb}	0.18 b_{fb}

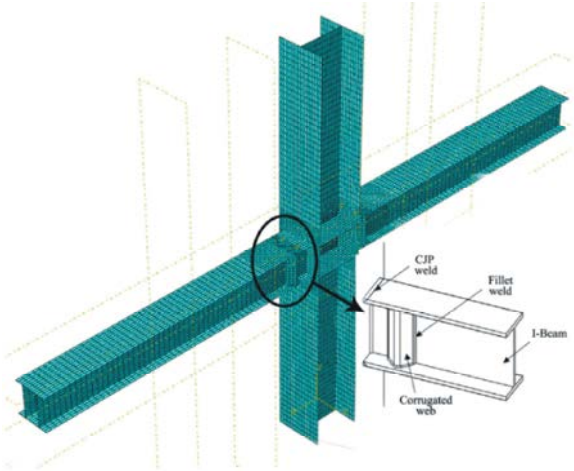

Fig. 2: AW-RBS configurations

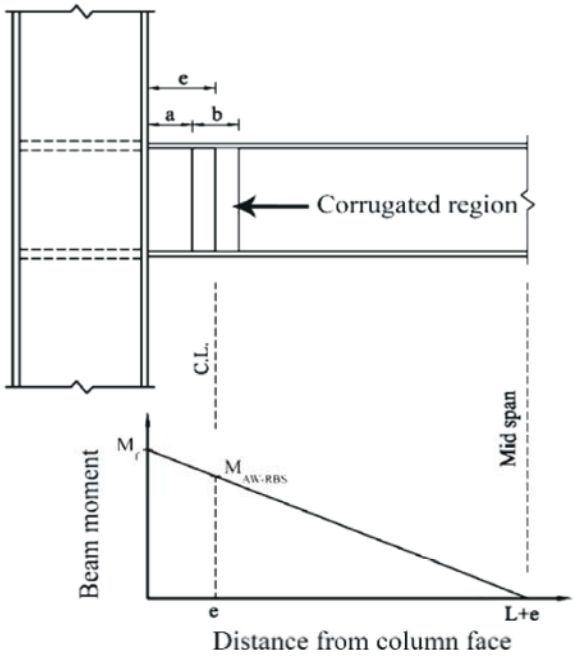

Fig. 3: Bending moment gradient for seismic loading

start (parameter a) and to the center of the corrugated region (parameter e), as shown in Figure 3. These design parameters are selected in accordance with AISC recommendations for radius cut RBS connections in order to obtain sensible trial values [23]. Accordingly, the distance to the reduced region (a) is 50-75% of the beam flange width (b_f) and the reduced region length (b) is 65-85% of the beam depth (d_b). The acceptable ranges of parameters *a* and *e* (*e=a+b/2*), based on the above values, are as follows:

$$a = (0.5 \text{ to } 0.75)\, b_{fb} \quad (1)$$

$$b = (0.65 \text{ to } 0.85)\, d_b \quad (2)$$

$$c \leq 0.25 b_{fb} \quad (3)$$

According to Eqs. (1), (2) and (3) the parameters a and b in all specimens are calculated. At the column face, the maximum moment should be smaller than the plastic moment of the beam in order to limit the possibility of fracture in the beam flange groove weld or surrounding heat affected regions. As shown in Figure 3, the maximum moment demand at the column face. (M_f) is calculated by projecting the maximum expected moment. (M_{AW-RBS}) developed at the center of reduced region to the column face as follows:

$$M_f = M_{AW-RBS}(L+e)/L \quad (4)$$

where L is the distance from the center of the reduced region to the point of inflection in the moment diagram. The maximum expected moment at the center of the reduced region, considering strain hardening, is as follows:

$$M_{AW-RBS} = 1.1 Z_{AW-RBS} F_{ye} \quad (5)$$

where Z_{AW-RBS} is the plastic section modulus of the corrugated region. It is calculated upon flanges only due to the accordion effect of the corrugated web and is equal to $2t_f\ b_f.(d_b\ -t_f)$, where t_f is the flange thickness. The expected yield strength, F_{ye}, is equal to R_yF_y; here, R_y is the difference between the minimum specified yield strength (F_y) and the expected yield strength. R_y of ST37 steel hot-rolled structural shapes is 1.5, in accordance with AISC [23]. Moreover, the multiplier 1.1 accounts for the peak connection strength including limited strain hardening and other types of over-strength, proposed in AISC [23].

Elements Used for Simulation: All the beams and columns are simulated using SHELL elements having bending in the ABAQUS element library. The beam properties are input by defining the relevant cross-sectional shape from the predefined ABAQUS cross-section library. At each increment of the analysis the stress over the cross-section is numerically integrated to define the beams response as the analysis proceeds. This allows the analysis to follow the development of the full elastic-plastic behaviour of the section at each integration point along the beam.

The steel beam to column connections is assumed to be fully resistant. The Doubler plate, Continuse plate and corrugated plate is simulated using with SHELL elements in the ABAQUS element library.

Materials Model of Steel: The model also incorporates non-linear material characteristics and non-linear geometric behavior. The material properties of all the structural steel components are modeled using an elastic-plastic material model from ABAQUS.

The incorporation of material non-linearity in an ABAQUS model requires the use of the true stress (σ) versus the plastic strain (ε^{pl}) relationship. This must be determined from the engineering stress-strain relationship. The stress-strains relationship in compression and tension are assumed to be the same in ABAQUS. The classical metal plasticity model defines the post-yield behavior for most metals. The material will behave as a linear elastic material up to the yield stress of the material. After this stage, it goes into the strain hardening stage until reaching the ultimate stress. As ABAQUS assumes that the response is constant outside the range defined by the input data, the material will continuously deform until the stress is reduced below this value.

The elastic part of the stress-strain curve is defined with the ELASTIC option, the value 2×10^7 (kg/cm^2) for the Young's modulus and 0.3 for Poisson's ratio are used. The plastic part of the stress-strain curve is defined with the PLASTIC option. The beams, columns, continuity plates and corrugated plates are all of ST37 steel with nominal yield stress of 240 Mpa.

Loading History, Testing Method and Instrumentation: In this research, the specimens were tested by imposing a prescribed quasi-static cyclic displacement specified in the AISC seismic provision [23]. The total story drift angle is calculated by dividing the exerted displacement by the column height. The loading history was of six cycles, each of 0.375, 0.5 and 0.75% total story drift angle, sequentially. The next four cycles were at 1% story drift, followed by two cycles each of successive increasing drift percentages (i.e., 2, 3, 4 . . . %). The cyclic tests are accomplished with a low rate for best monitoring the responses of the specimens as well as their deformations during the loading history. Figure 4 shows step test and deformation parameter and inter-story drift angle.

Boundary Condition and Mesh Size: The models are supported at the bottom as shown in Figure 5. The mesh representing the model has been studied and is sufficiently fine in the areas of interest to ensure that the developed forces can be accurately determined.

Validation of the Model: In order to valid the proposed models. The testing model of seismic performance of the Accordion-Web RBS connection was applied by Mirghaderi *et al*. [21]. The model was set up based on the same modeling techniques discussed in this paper. The model size, connections and boundary conditions are exactly the same as the full sale tests [21].

For the Accordion-Web RBS connection was defined as fixed. The same material properties of the test were defined using the material function of ABAQUS for models. Figure 5 shows the modeling results of moment rotation relationship of the Accordion-Web RBS connection with ABAQUS, compared to the moment rotation relationship of the Accordion-Web RBS connection of Mirghaderi *et al*. [21]. It can be seen that, good agreement is achieved in the initial stiffness and yield strength. However, for the proposed model, it can predict less rotation capacity after yielding.

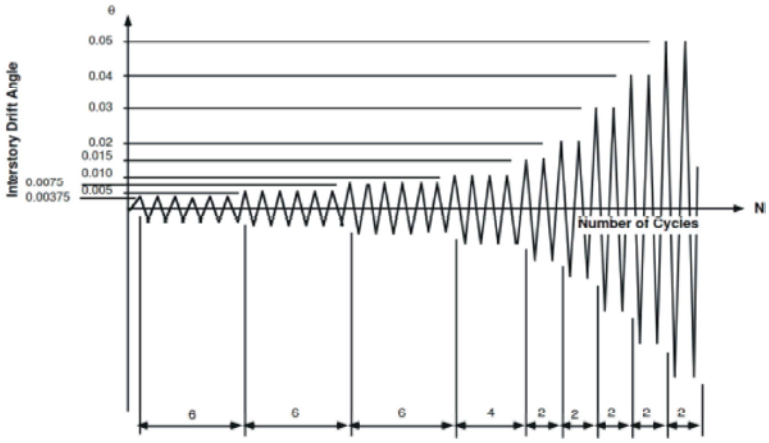

Fig. 4: Multiple Step Test, Deformation Parameter is Inter-story Drift Angle

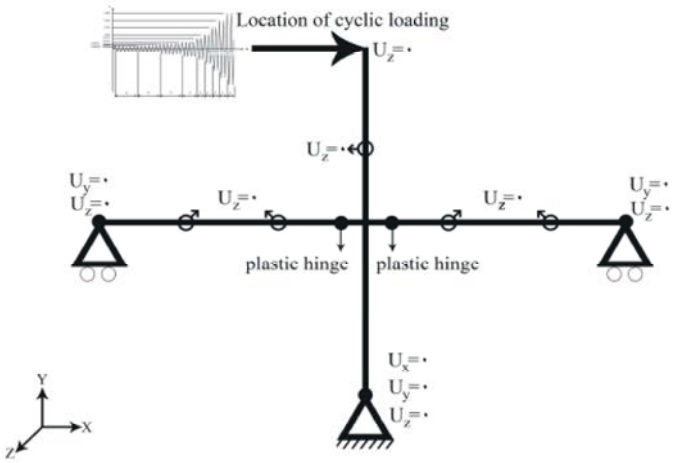

Fig. 5: Load and the boundary condition of the numerical model

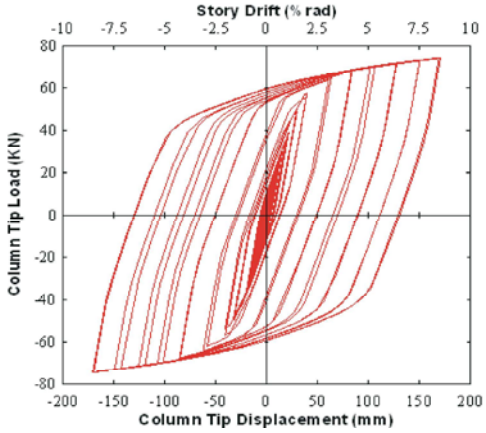

Fig. 5: The finite element cyclic results

Analytical Study of the Connection Behavior: The connection's cyclic behavior has been I nvestigated. The cyclic response, the plasticization pattern, the behavior of the reduced region and other components of the connection are analyzed and compared with themselves for better understanding of the seismic behavior of the RBS and AW-RBS connections.

As seismic performance of connections in seismic load is partially dependent on panel zone, it is preventing the failure with reinforced panel zone. The cyclic responses of the RBS with radius-cut, predicted analytically, as shown in Figures 6 and 7. No degradation is observed in the hysteretic responses of specimens throughout the finite element analysis.

However, yielding of elements occurred during 1.5% story drift in the weakened zone. Local buckling of the beam flange occurred during 5% story drift, leading to a decrease of the hardening slope and a flattening of the curve during the last cycles. Hysteretic behavior of the RBS with radius-cut is similar to the RBS with triangular-cut, as shown in Figures 8, 9, 10 and 11 models is cutting geometry. Due to trapezoidal geometry cut, stress concentration and local buckling of the beam flange

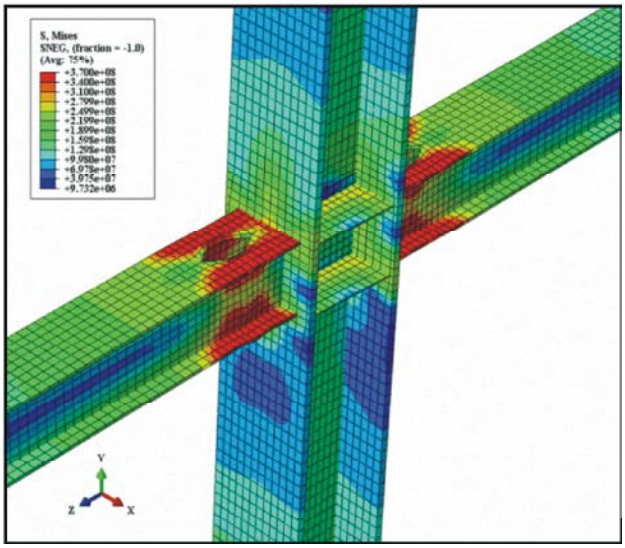

Fig. 6: Von Mises plastic stress distribution at 6% story drift

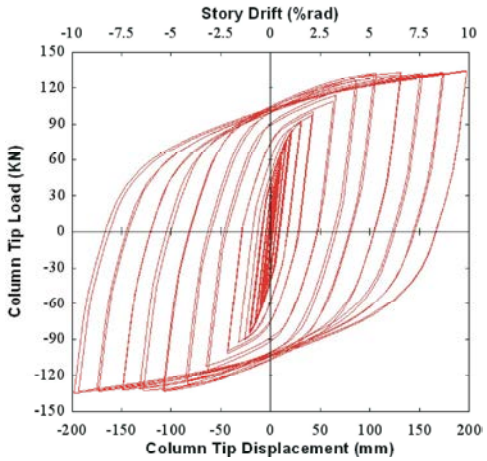

Fig. 7: Load versus column tip displacement (and story drift angle)

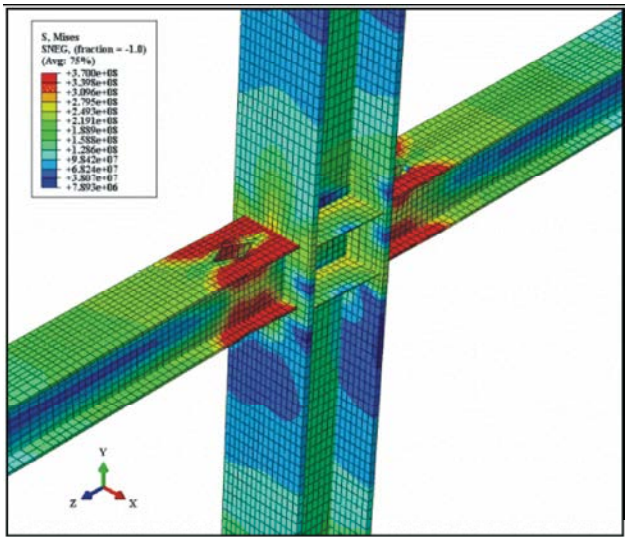

Fig. 8: Von Mises plastic stress distribution at 6% story drift

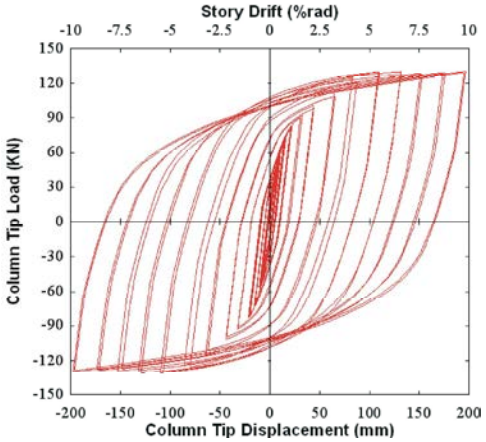

Fig. 9: Load versus column tip displacement (and story drift angle)

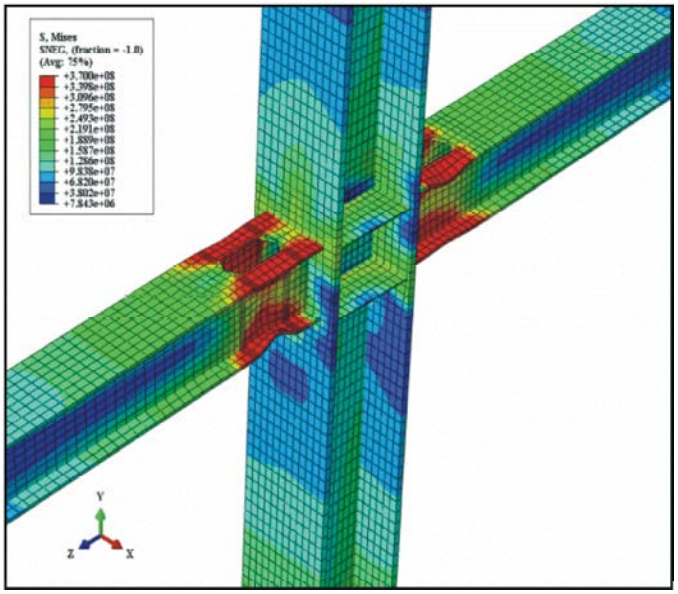

Fig. 10: Von Mises plastic stress distribution at 6% story drift

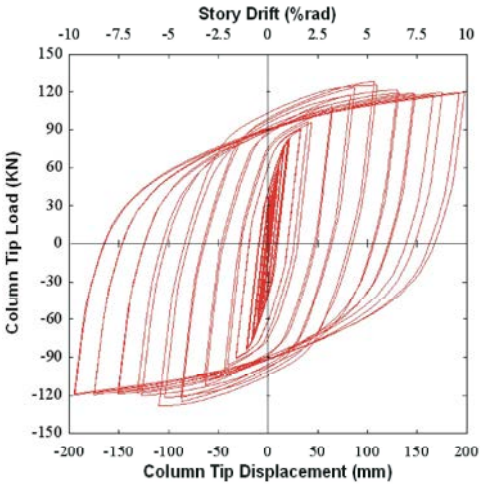

Fig. 11: Load versus column tip displacement (and story drift angle)

occurred in the RBS with trapezoidal-cut and more unstable than of the RBS with radius-cut and triangular-cut.

The cyclic responses of the Accordion-Web RBS with double I-beam, is shown in Figures 12 and 13.

The first yielding of element in the Accordion-Web RBS emerged after the cyclic loading at the center of the corrugated region during the first cycle of 1.5% story drift cycles. The yielding was more apparent after 2% story drift cycles. It was spread over the entire reduced region during 3% story drift, while no sign of yielding was observed in the corrugated web and the beam outside the reduced region.

The flange yielding was extended toward the column face and beam end during the first cycle of 4% story drift. The yielding patterns continued during 5 and 6% story drift cycles; the yielding was more extended to both sides of the corrugated region and it became nearly apparent outside the corrugated region, near the column face. In addition, plastic hinges are completely formed during 5% story drift in the predefined reduced region and the plastic deformations are concentrated therein.

Here, a flange local buckling was detected before the corrugated region in both beams following the first cycle of 7% story drift. Furthermore, a lateral flange movement commenced at the end of the second cycle in the right beam. This was followed by the onset of the beam web buckling, although its amplitudes were very small. The amplitude of buckling increased in the first cycle of 8% story drift and during the second cycle. The yielding at the corrugated web corners extended into the beam depth on both sides of the specimen as well as the connection line of the corrugated plates to the flat web. Furthermore, based on the analytical results, the plastic strains are about one fifth of the strain near the column face. The local plastic strains at the corners of the corrugated plates showed brittle failure potential.

The cyclic responses for specimens of the RBS with weakened web and used corrugated plate on the inside and outside of specimens, as shown in Figures 14, 15, 16 and 17. According to the results, plastic hinges are completely formed during 3% story drift in the predefined reduced region.

The cyclic responses for specimens of the AW-RBS with double I-beam and with section IPE140, IPE160, IPE180, IPE200, IPE220, is shown in Figure 18.

According to the results, increase the beam section with constant the column section to a certain extent responsible for the connection. Additionally, dependent on parameters of the beam such as the thickness flange, web, width flange and etc cannot be considered independently. This formula can be proposed for the seismic control steps of the AW-RBS connections.

$$\frac{Z_{AW-RBS}}{Z_b} \leq 20\% \quad (6)$$

where $Z_{AW\text{-}RBS}$ is the plastic section modulus of the corrugated region and Z_b is the plastic section modulus of the Beam.

The deformed shape and the plastic strain distribution of the RBS and AW-RBS model are shown in Figures 19 and 20 at 6% story drift. According to the results, plastic hinges are completely formed in the predefined reduced region and the plastic deformations are concentrated. The development of a reduced region and the concentration of plastic strains, in this region were observed through the simulation as shown in Figures 21 and 22 demonstrate the envelope of vertical profile of axial strain in the plastic hinge in the corrugated web and beam flange for the RBS with radius-cut and the Accordion-Web RBS. According to this figure, the top flange strains are substituted for the bottom ones at the reduced region center, assuming the top and bottom flange strains to be nearly equal. As depicted in the figure, the axial stress is negligible along the beam axis in the corrugated web compared to the flange strains excepted for web areas near the beam flange because of the local effects of the beam flanges.

The formation of a plastic hinge at the reduced section can also be demonstrated by means of a longitudinal strain profile along the beam top flange, as shown in Figures 23 and 24. The formation of the plastic hinge in the predefined region is confirmed by higher values of normalized strain, developed in the flanges within the reduced section. According to Figures 23 and 24, the strain values at the reduced section are over three times the strains near the column face. The demand of plastic strains is decreased near the column face. According to the curves, the first yielding in the plastic hinge is in 1-1.5% story drift cycles in both specimens. Therefore, plastic hinges are completely formed in both specimens at the end of 4% story drift. It should be noted that the inherent flange and web local buckling potential are eliminated at the plastic hinge location by means of the corrugated web and the buckles occur before the corrugated region, as seen during the final cycles of the modeling.

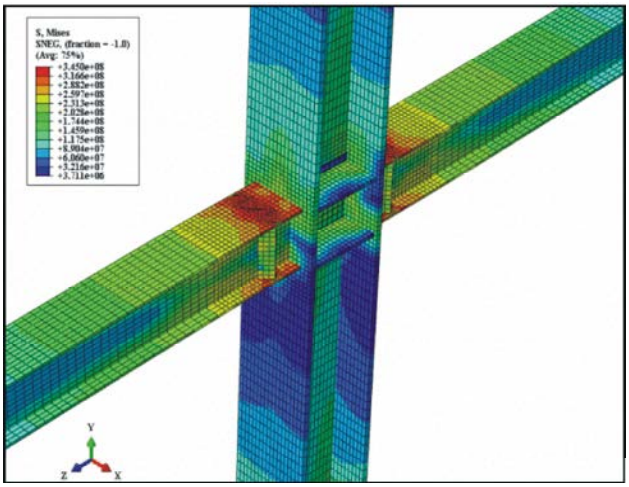

Fig. 12: Von Mises plastic stress distribution at 6% story drift

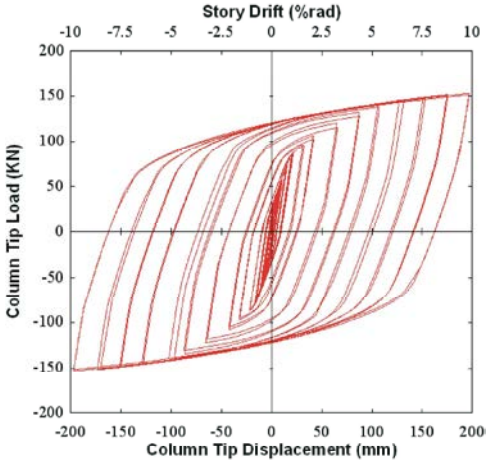

Fig. 13: Load versus column tip displacement (and story drift angle)

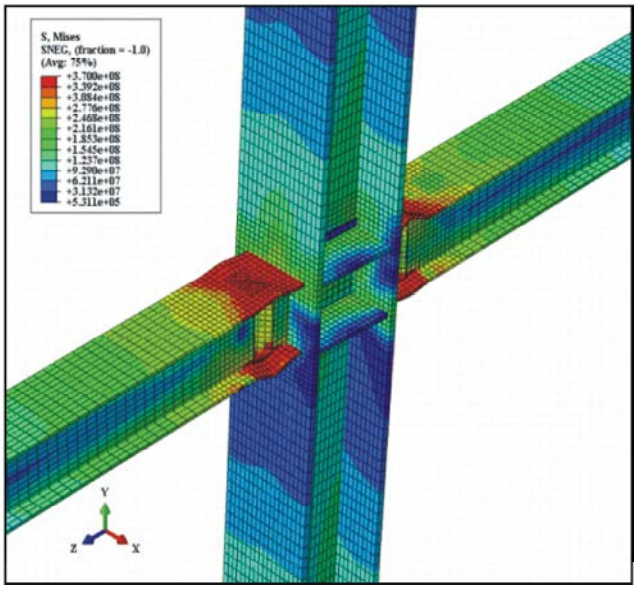

Fig. 14: Von Mises plastic stress distribution at 6% story drift

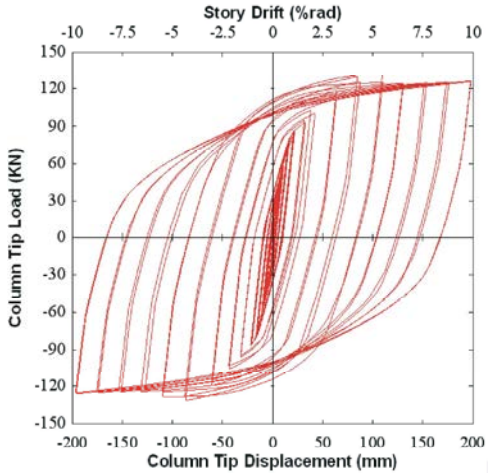

Fig. 15: Load versus column tip displacement (and story drift angle)

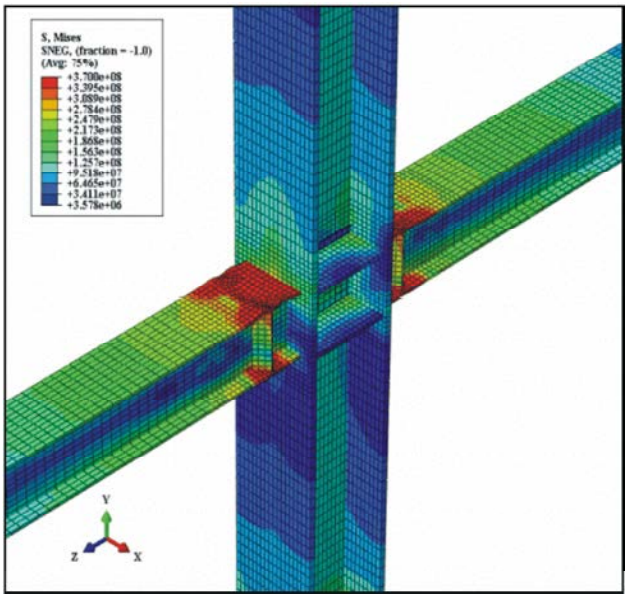

Fig. 16: Von Mises plastic stress distribution at 6% story drift

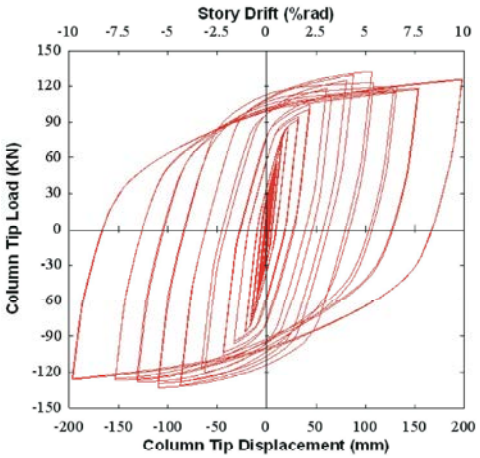

Fig. 17: Load versus column tip displacement (and story drift angle)

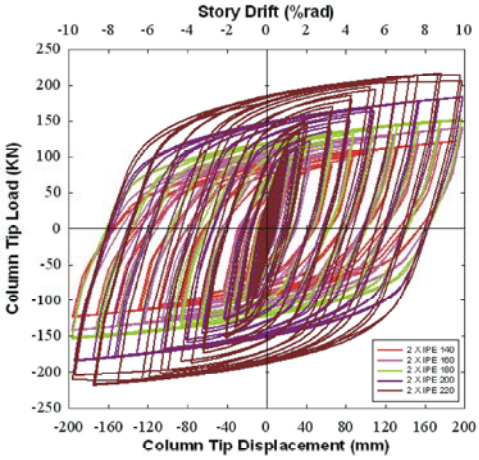

Fig. 18: Load versus column tip displacement (and story drift angle) for different profile with AW-RBS connections

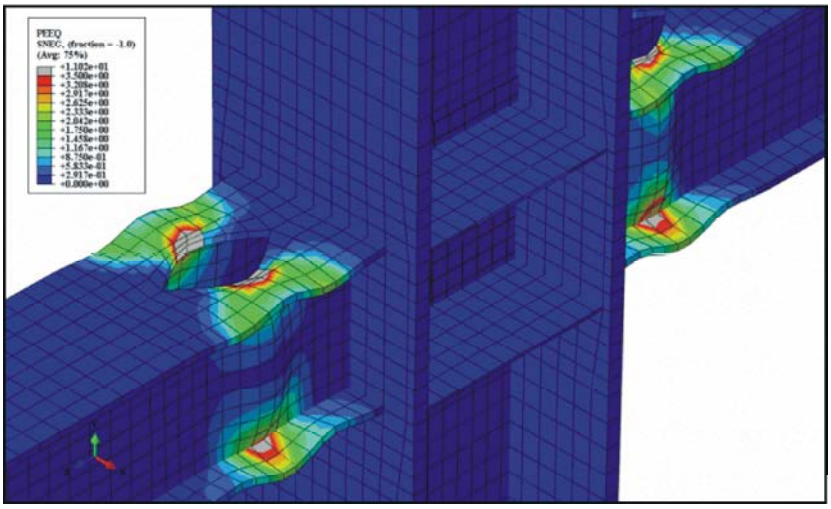

Fig. 19: Equivalent plastic strain distribution in the radius-cut RBS connection

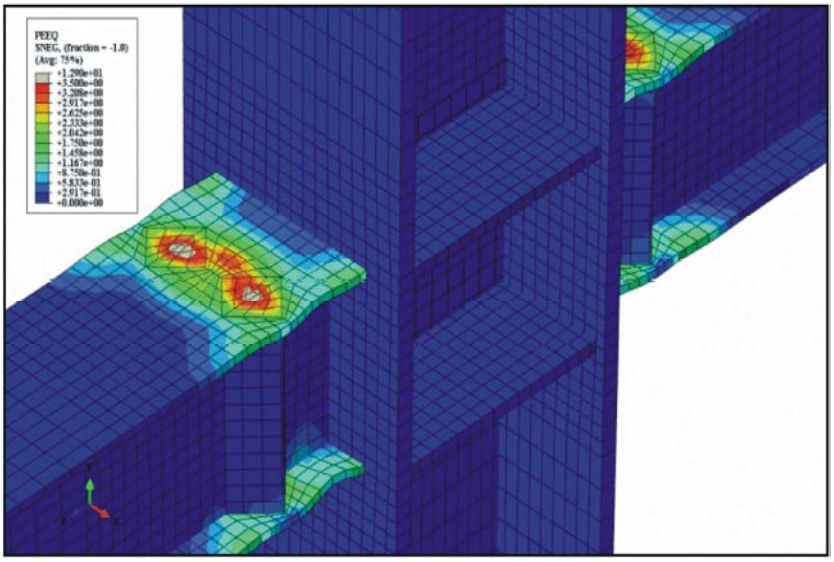

Fig. 20: Equivalent plastic strain distribution in the AW-RBS connection

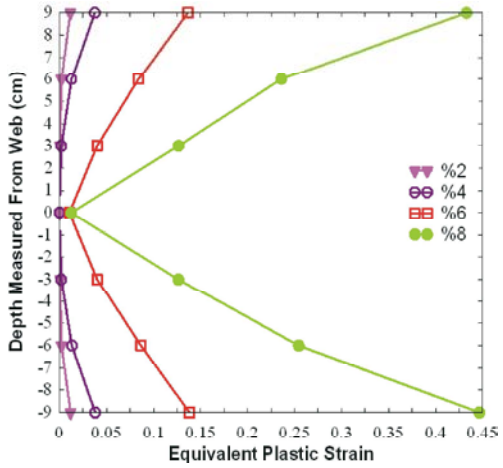

Fig. 21: The vertical profile envelope of axial strain for AW-RBS connection

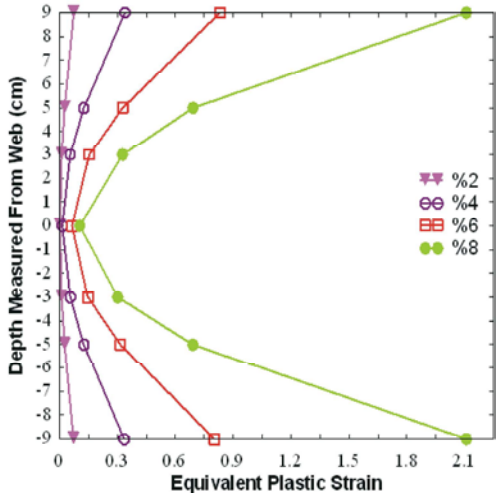

Fig. 22: The vertical profile envelope of axial strain for the radius-cut RBS connection

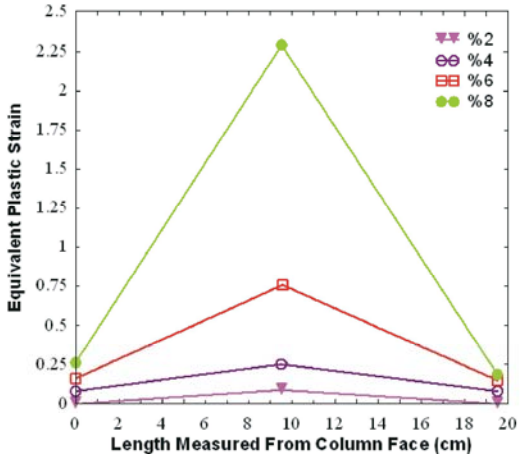

Fig. 23: The strain profile along the beam top flange for the AW-RBS connection

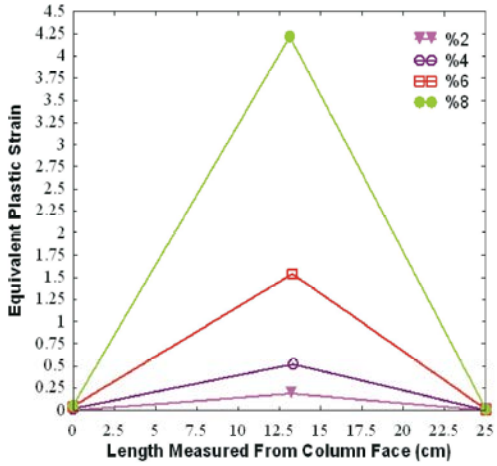

Fig. 24: The strain profile along the beam top flange for the radius-cut RBS connection

From the comparison of RBS and AW-RBS, it can be seen that the connections is more vulnerable to the RBS of the AW-RBS. Generally, the yielding and buckling patterns of the Accordion-Web RBS model are in good agreement with typical RBS model results. Additionally, the accordion effect of the corrugated plate is precisely studied by the finite element analysis.

CONCLUSIONS

In this paper, a 3-D finite element model was first built with the ABAQUS package to simulate the seismic behavior of the RBS and Accordion-Web RBS connection. The methodology for the modeling techniques is described in details. The model also incorporates non-linear material characteristics and non-linear geometric behavior.

Using the proposed model, the seismic behavior analysis of 10 specimens with different lateral geometry cut was investigated. The main findings are summarized as follows:

- As the occurrence of flange buckles is deferred by the corrugated plates, reliable and stable plastic hinge behavior is obtained in AW-RBS compared to RBS connections.
- According to the analytical results, the inelastic rotations are mostly provided by reliable and ductile plastic hinge rotation of the AW-RBS compared to RBS connections.

- Due to strength loss for more than 8% story drift angle in the cyclic tests shows that the nonlinear rotation capacity of the AW-RBS connection is in excess of the current requirements for qualifying connections in special moment frames.
- Based on the seismic observations results, we need to seismic control the AW-RBS connection with column IPB profile and beam IPE profile by equation 6, for the prevention of formation plastic hinge in the column and panel zone.

REFERENCES

1. Plumier, A., 1990. New Idea for Safe Structures in Seismic Zones. Proc. IABSE Symposium - Mixed Structures Including New Materials, Brussels, Belgium, pp: 431-436.
2. Carter, C.J. and N.R. Iwankiw, 1998. Improved ductility in seismic steel moment frames with dogbone connections. Journal of Constructional Steel Research, pp: 253-258.
3. Chen, S.J. and C.T. Tu, 2004. Experimental study of jumbo size reduced beam section connections using high-strength steel. Journal of Structural Engineering, ASCE, 130(4): 582-587.
4. Rothwell, A., 1968. The shear stiffness of flat sided corrugated webs. Aeronotical Quarterly, 19(3): 224-34.
5. Sherman, D. and J. Fisher, 1971. Beams with corrugated webs. In: Proc. 1st spec. conf. on cold-formed steel structures. Rolla (MO): Univ. of Missouri-Rolla, pp: 198-204.
6. Libove, C., 1973. On the stiffness, strength and buckling of corrugated shear webs. In: Proc. 2nd spec. conf. on cold-formed steel structures. Rolla (MO): Univ. of Missouri-Rolla, pp: 259-301.
7. Libove, C., 1977. Buckling of corrugated plates in shear. In: Proc. int. colloquium on struct. stability, struct. stability res. council. Bethlehem (PA): Lehigh Univ., pp: 435-62.
8. Easly, J.T., 1975. Buckling formulas for corrugated metal shear diaphragms. Journal of Structural Engineering ASCE, 101(7): 1403-17.
9. Wu, LH. and C. Libove, 1975. Curvilinearly corrugated plates in shear. ASCE Journal of Structural Engineering, ASCE, 101(11): 2205-22.
10. Hussain, M.I. and C. Libove, 1977. Stiffness tests of trapezoidal corrugated shear webs Journal of the Structural Division, ASCE, 103(st5).
11. Harrison, J.D., 1965. Explaratory fatigue tests of two girders with corrugated webs. British welding Journal, London, England, 12(3): 121-5.
12. Korashy, M. and J. Varga, 1979. Comparative evaluation of fatigue strength of beams with web plate stiffened in the traditional way and by corrugation. ACTA technica academiae scientiarum hungaricae, Tomus, 89: 309-46.
13. Bergfelt, A. and L. Liva-Aravena, 1984. Shear buckling of trabizoidally corrugated girder webs. Rep. No. S 84-2. G ¨ oteborg (Sweden), Dept. of Structural Engrg: Chalmers University of Technology.
14. Lindner, J. and R. Aschinger, 1990. Torsional stiffness of welded I-girder with trapezoidally corrugated webs. Germany: Technische Universitat berlin, Frachgebiet Stahibau, Sekr. Bl.
15. Scheer, J., H. Pasternak, K. Plumeyer, J. Ruga and O. Einsiedler, 1991. Trapezstegr¨ ager Geschweibt. Rep. No. 6203. Germany: Institut f¨ ur Stahlbau, TU Braunschweig.
16. Hamada, M., K. Nakayama, M. Kakihara, K. Saloh and F. Obtake, 1984. Development of welded I-beam with corrugated web. The Sumitomo Search, Tokyo, Japan, 29: 75-90.
17. Heywood, P., 1987. Corrugated box-girder web lowers bridge weight and cost. ENR, pp: 23-28.
18. Combault, J., 1988. The Maupe Viaduct Near Charolles France. In: Proceedings of the AISC Engineering Conference, 12-1-12-22.
19. Elgaaly, M. and H. Dagher, 1990. Beams and girders with corrugated webs. In: Proceeding of the annual technical session. Bethlehem (PA): Structural Stability Research Council (SSRC) Lehigh Univ., pp: 37-53.
20. Chan, C.L., Y.A. Khalid, B.B. Sahari and A.M.S. Hamouda, 2002. Finite element analysis of corrugated web beams under bending. Journal of Constructional Steel Research, 58(11): 1391-406.
21. Mirghaderi, R., S.H. Torabian and A. Imanpour, 2009. Seismic performance of the Accordion-Web RBS connection. Journal of Constructional Steel Research.
22. Karlsson and Sorensen, 2011. ABAQUS theory manual, Version 6.11 Hibbitt. Pawtucket (RI).
23. AISC/ANSI 358-05., 2005. Prequalified connections for special and intermediate steel moment frames for seismic applications specification. Chicago (IL): American Institute of Steel Construction.